International Conference on
RESEARCH IN
MECHANICAL ENGINEERING
15 December 2016 Singapore
www.rmeconf.com

Analysis of thermal performance In an industrial furnace using CFD

Oveis Alizadeh Shoeili
Mechanics, Urmia University, Tehran, Iran
Oveyssh.2010@yahoo.com

Yaser Moghaddam
Chemical Engineering, Ferdowsi University Of Mashhad, Tehran, Iran
Ymoghaddam65@yahoo.com

Amin Balazadeh Kouche
Aerospace Engineering, Khaje Nasir University of Technology, Tehran, Iran
Balazadeh.aero@yahoo.com

Abstract
The Detailed numerical simulations are used to estimate the thermal behavior of an industrial furnace (an aluminum holding furnace) heated by a system of electrical resistances. Estimated temperatures are compared with experimental measurements taken in a real prototype. As a first approach, the symmetry of the geometry is used to reduce the computational resources and only a quarter of domain is initially simulated. Nevertheless the predicted velocities for the flow in the molten load suggest that the patterns induced by the convection effects have a three dimensional behavior. For this reason a new simulation with the full domain is carried out. Both simulations predict almost the same temperatures and energy distributions with different patterns of flow in the molten load. Chaotic behavior is predicted by the full domain approach for the movement of the aluminum bath, which corresponds to problems of natural convention with small differences in temperature and density due to the high thermal conductivity of the material. Although the effects on the thermal performance are very small or even undistinguishable, variations in the movement of the molten load may affect other aspects, such as for instance, the metallurgical properties of the final products.

Keywords: CFD, Industrial furnace, Thermal performance

Introduction

In aluminum secondary production, the metal is recovered from new and old scrap. The load is melted in different furnaces and process and the molten load is transferred to holding furnaces, where its temperature is maintained or increased and its composition is adjusted for the casting process. The use of a holding furnace makes it possible to operate the melting furnace under conditions that most favor heating of solid scrap, improving the efficiency and melting rate. It is highly desirable that the molten metal remains at a homogeneous temperature, which is in many cases very difficult to execute especially by means of combustion. In fact, the utilization of electric holding furnaces has increased due to their ability to control the temperature and composition of the load.

Several furnace types are used in the aluminum holding process; the most frequently used are reverberatory or crucible furnaces heated by electrical resistances, gas-fired or radiant pipes; designs include heating from the top of furnace, lateral walls or immersed pipes. Induction furnaces are used also in the holding stage, but are much more expensive per unit load capacity than fossil-fuel furnaces.

In spite of the evolution of the numerical techniques and the increase of the computational resources, the use of Computational Fluid Dynamics (CFD) is not a methodology commonly used by manufacturers of industrial furnaces, whose designs continue to be based on semi-empirical methods. Numerical approaches are usually limited by strong simplifications; some of the challenges that have prevented the intensive use of computational techniques in this area are the radiation heat transfer, interactions gas liquid solid, and conjugated heat diffusion, movement of the molten load, 3D geometries and heating means. Additionally, the load material can present solidification depending on time and space, when the heat supply is not enough.

Due to these difficulties only few publications report numerical simulation of holding furnaces. The following works can be quoted as direct background: Wang et al. [1] present an optimization process for an aluminum holding furnace based on a combination of CFD study, a response surface methodology and an uniform design. For the CFD study, a three dimensional model focused in the combustion chamber was accomplished, the energetic interaction with the molten load was taken into account, but the furnace is simplified as a non-conjugate problem and the momentum equations are not solved for the molten aluminum. A similar approach was adopted previously by Zhou et al. [2] for a stationary problem. Pauty et al. [3] present numerical simulations of holding and tilting processes; during the holding, the conjugated problem is solved in 2D under the assumption of steady state; the heating is performed by a boundary condition of fixed temperature at the top of the molten load. Although the density of the molten aluminum is treated with the Boussinesq approximation, the load flow field never converged due to numerical oscillations and this is attributed to a source of turbulence that not was taken into account. Darwish [4] uses simplified correlations in order to model heat transfer in an aluminum holding furnace model as a 2D conjugated problem; the results predict a difference of the load temperature which is attributed to the shape of the furnace. Blakey and Beck [5] present a numerical simulation of a galvanizing furnace, which is a device similar to the holding furnace, since it is designed to maintain the molten zinc at a fixed temperature. The work focuses on the interaction of the combustion gases with the walls of the furnace that contains the molten bath.

Of course, many other types of furnaces have been analyzed. Examples of recent works are the following. Martín et al. [6] present two models to estimate the behavior of a heat treatment furnace for steel pieces. The first is a numerical approach that uses the finite element method in a 2D steady-state assumption. The second model is a 2D transient approach that interpolates the results of numerical simulations in a database for different operating conditions and it is used to estimate the heating process of the steel pieces. Predictions of the reduced model are used in order to optimize the natural gas combustion. Mooney et al. [7] develop a simplified 1D numerical model to estimate the heat transfer in a Bridgman furnace. The load material is a titanium aluminide based, multi-component alloy and the phase change in the process is considered dominated by heat conduction. This study uses experimental measurements of temperature to determine the heat flux and heat transfer coefficients that are used in a reduced thermal model. Carmona and Cortes [8] have presented a numerical simulation of an aluminum melting furnace; they conclude that for a complete analysis of the heat losses in the furnace, it is necessary to take into account all the interactions gas liquid solid. This kind of detailed simulation has not been presented in bibliographic references so far for holding furnaces. In

addition, the shortcomings of the current measurement techniques in this context do not allow a comprehensive characterization of the equipment operation. Accordingly, a great deal of information is missing about this kind of devices.

In this paper, comprehensive 3D CFD numerical simulations are developed in order to reproduce a typical operation cycle of an aluminum holding furnace. Preheating of the furnace is the most important process involved since the high temperatures reached by the walls and the heat stored in the refractory parts are used for holding the load; simulations are focused on the unsteady heat transfer process of this device where the input power is performed by an on off control. The holding furnace analyzed, assumptions, models and methodology employed are presented below. Also, results and comparison with experimental measurements are discussed in detail.

Experimental configuration

Prototype description

The main aim of the prototype is to maintain the aluminum above its melting temperature, transferring heat to the load in a homogeneous form and reducing the contamination in the molten metal. The furnace consists of a composite of different refractory materials, which enclose a holding chamber and a heating chamber separated by a refractory layer. An array of electrical resistances is located in the heating chamber. The holding furnace was designed to kept aluminum in the range of 680-800 [C]. A sectional view of the analyzed furnace at the center plane is shown in Fig. 1(a), while the main dimensions are shown in Fig. 1(b).

In addition to the materials shown in Fig. 1, two thin layers of material are located on the outer surface of the lateral walls of the furnace: a ceramic layer used as a supplementary insulation (6 mm thickness) and a sheet of steel 1018 used as a protection for the refractory materials (5 mm thickness).

Measurements

The molten temperature is measured with a submerged thermocouple protected by a steel tube. Air temperature inside the heating cavity is measured through thermocouple probe. The internal temperatures of the refractory walls are measured through an array of thermocouples in three points at a height of 150 mm from the top of the furnace. Estimated uncertainty of measurements is ±2 K. The locations of these instruments in the experimental rig are shown in Fig. 1, marked as T1eT5.

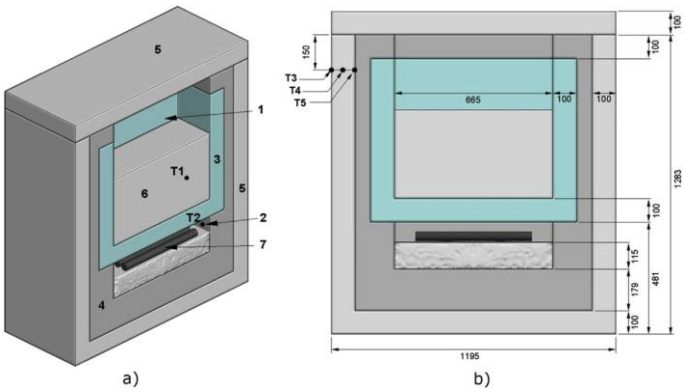

Fig. 1. a) Sectional view of the aluminum holding furnace (1-holding chamber, 2-heating chamber, 3-layer of refractory material A, 4-layer of refractory material B, 5-layer of refractory material C, 6-aluminum load, 7-electrical resistances, T1-thermocouple in load, T2-thermocouple in heating chamber); b) main dimensions in mm (T3 to T5-thermocouples in walls)

Test protocol

The holding furnace is preheated by the electrical resistances from the ambient temperature (291 K) until the refractory walls reach the operation temperature and the furnace becomes stable (12-15 days). The high temperatures of the refractory walls are used to maintain the load above the melting point. Molten aluminum is poured into the holding chamber and it is held for several hours. The power supply is controlled to compensate the heat losses from the furnace by a simple on off control, which introduces a constant power until the resistances chamber reach a maximum operation temperature and then is turned off until a minimum operation temperature.

Model description

Assumptions and boundary conditions

The commercial CFD code FLUENT is used to accomplish the numerical simulations. For the spatial discretization, the first-order upwind scheme is adopted. The SIMPLE algorithm is used for pressure velocity coupling and the standard scheme is applied for pressure interpolation. The convergence strategy used is a decrease of the absolute residuals in each time step of 1e-3 for the continuity and momentum equations, and of 1e-6 for the energy equation. The user's manual ANSYS [9] gives details of the numerical techniques.

It is assumed that the metal load of 250 kg fills the holding chamber uniformly up to a specific height. The domain is considered closed without air infiltrations. Due to thermally induced density differences, the air and molten load move in the holding chamber. Rayleigh numbers can be estimated as 8-5 and 5-7. The first is relatively far to the turbulence transition value of 10^9 typically quoted for external flows in air [10], and turbulence transition of liquid aluminum in confined spaces is not clearly established. Therefore, in order to reduce the computational resources required, laminar flow is assumed for both air and load sub-domains.

Treatment of air convection and surface radiation in the resistances' chamber is based in a purely diffusive transfer in quiescent air, with an augmented, effective thermal conductivity given by $k_{eff} = h_{eff}t$. Since details of the temperature distribution in the air filling the cavity are of no concern, this approach is used in order to save computational resources, see Carmona and Cortes [8]. The chamber is considered as a box with an array of cylinders that represent the electrical resistances, with a height equal to the distance between the resistances and the top (in this case: t = 61 mm), and uniform surface temperatures of 1473 K for the resistances and 1073 K for the top and lateral walls. Using basic heat transfer calculations [11] coefficients are $h_{conv} \sim 3.5$ W/ (m^2 K), $h_{rad} \sim 231.7$ W/ (m^2 K), $h_{eff} = h_{conv} + h_{rad} \sim 235.2$ W/ (m^2 K), and the augmented air conductivity $k_{eff} = 14.35$ W/ (m K).

Heat losses from the external walls to the surroundings are computed as follows. A perfect insulation is considered at the bottom of the furnace. Lateral walls of the furnace are composed by two sheets of different materials: 1) A ceramic fiber layer, which is the final material in the refractory array. 2) A sheet of steel 1018. Both sheets have very small thickness in comparison with the other materials and thus would force an exaggerated grading of the mesh, which may lead to numerical convergence problems. In order to represent heat conduction avoiding this problem, a thin-wall model is used. In this model, conduction along the thin wall is neglected and the ensuing locally 1D conduction in the transversal direction results in a thermal resistance given by $\Delta x/k$, where k is the conductivity of the wall material and Δx is the wall thickness. Fig. 2 summarizes the treatment of the outermost part of the wall. Conduction heat transfer in material C (see Fig. 1) is fully modeled by the CFD code, and its surface heat flux coupled to the thin-wall model. Since the latter is restricted by the code to only one material, an equivalent series thermal circuit is considered for the two layers as $keq = k_{Cer}k_{Steel}(t_{Cer}+ t_{Steel})/ (t_{Cer}k_{Steel} + t_{Steel}k_{Cer}) = 0.26$ W/ (m K).

Finally, natural convection and radiation heat transfer to environment is modeled by a constant, average heat transfer coefficient $h_{av}= h_{conv} + h_{rad}$ [W/ (m^2 K)], that can be obtained from basic heat transfer calculations [11]. h_{conv} is estimated applying an empirical correlation for vertical walls. The formula of losses to a large (thus, black) radiative environment is used in order to estimate h_{rad}. For the

calculation of these coefficients, temperature of the walls and surroundings are considered uniform and known, with representative values of 523 K and 291 K, respectively. Total emissivity used is a typical value of 0.7 for non-polished surfaces. Calculation results in $h_{conv} \sim 7$ W/ (m^2 K), $h_{rad} \sim 11$ W/ (m^2 K), and thus $h_{av} \sim 18$ W/ (m^2 K).

The electrical resistances supply a total constant input power (W_{input} = 11 kW) until the heating chamber reaches a temperature of 1273 K, then these are turned off until the temperature in the heating chamber drops to 1268 K. The resistances are simplified as an array of cylinders. Since the internal temperature of the resistances is not of interest for the present simulations, the heat generation is imposed as a boundary condition in the surface of the cylinders; which is in fact the power input in the furnace: $w = W_{input}/NA_{res} = 28356.08$ [W/m^2]. Where N is the number of resistances and A_{res} is the unitary area.

The on off control condition has been imposed in the resistances area by means of a User Defined Function (UDF) in FLUENT.

Geometry and materials

In order to reduce the computational cost and take advantage of the symmetry, only a quarter of the domain was simulated in a first approach. Since strong asymmetry was observed in the natural flow within the load, the full domain was simulated afterward to compare the results obtained by both approaches. Fig. 1 shows the geometry of the furnace simulated.

The resistances used in the furnace are wire elements of the typical material “aluchrom”. Table 1 shows the thermal properties for the solid parts in the furnace, while the thermo-physical properties of the aluminum load are summarized in Table 2.

Table1. Thermal properties of solid parts.

Material	Density, kg/m^3	Specific heat, J/(kg K)	Thermal conductivity, W/(m K)
Refractory material A	2563	690	8
Refractory material B	1200	1200	0.2
Refractory material C	930	1200	0.28
Ceramic layer	160	1088	0.143
Aluchrom	7100	640	16
Steel 1018	7800	489	50

Table 2. Thermo physical properties of aluminum load.

Density (kg/m^3)	2700	T < 873 K
Specific heat (kJ/kg K)	-3.873T + 5992 -0.3116T + 2668 0.900	873 K < T < 933.15 K T > 933.15 K
Thermal conductivity (W/m K)	237	
Viscosity (kg/m s)	0.001	
Latent heat of fusion (kJ/kg)	397	
Solidus temperature (K)	873	
Liquidus temperature (K)	933.15	

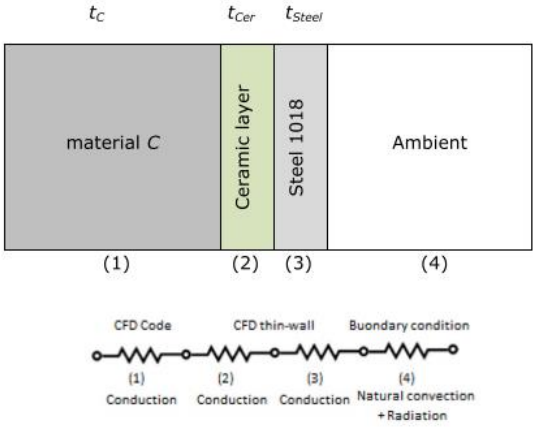

Fig. 2. Thermal circuit scheme in the lateral walls of the crucible.

Models

For the convective motion of the molten load and air filling up the holding chamber, the Navier-Stokes equations corresponding to a fluid of variable density are solved; this includes buoyancy. For all interfaces the non-slip condition is implemented. The energy equation is solved for all domains, enforcing the continuity of the temperature and the heat flux through interfaces.

Due to the solidification potential of the molten aluminum, a model to consider the phase change must be included in this kind of simulations. In this process, a moving boundary that separates the liquid and solid phases is generated. The location of this boundary is variable in time and can't be determined in advance. Carmona and Cortes [8] give a summary of the different methodologies applied to phase change problems, covering numerical techniques based in variable and fixed grid methods. The fixed grid enthalpy method [22, 23] is the most appropriate for simulations in industrial furnaces. Here, it is used in the load domain in order to detect possible solidification points.

In the air cavity, radiation heat transfer contributes significantly to heat losses, adding up to natural convection. In the present problem, only radiation between internal surfaces of the cavity, including inner furnace walls and top surface of the load must be considered. This is so because air inside the chamber is transparent, and aluminum (solid and liquid) is opaque to thermal radiation in the spectral range corresponding to the process temperature. Thermal radiation is computed with the so-called "surface-to-surface" (S2S) radiation model of FLUENT [9]. This is an integrated application of the net radiation method [10], coupled to the diffusive term of surface energy balances. In this method, the geometrical view factors between participant surfaces are first computed, only dependent on discretization. Also, diffuse-gray radiation is considered, which is realistic in the conditions of the furnace.

Mesh

The diversity of models considered in the numerical simulation demands large computational resources. As a result, it is not possible to accomplish a grid convergence analysis with the current capacities. A mesh of 531,150 cells and a mesh of 2,124,600 cells are used for the approaches of a quarter and full domain, respectively. The whole mesh is structured except in the heating chamber that has a complex geometry. Fig. 3 shows the general grid and details of the heating chamber for the case of the quarter of domain; this mesh is reproduced in each symmetry plane for the full domain.

Numerical time step

The problem complexity increases by two factors: first, after the preheating process, a new material is added to the domain (molten load); second the on off control prevents the use of a large value for the time step. Since in actual conditions the resistances are switched each 10-20 s approximately, the maximum time step used in the simulations is 3 s. Iterative convergence at each time step is verified. Trial tests show not dependence of the results with the time step used in a broad range.

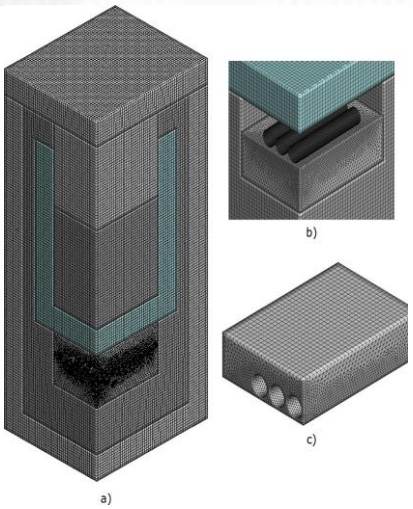

Fig. 3. Grid details-quarter of domain. a) General, b) resistances, c) air filling the resistances chamber.

Results and discussion

Pre heating stage

The preheating process is simulated in the first place. Once this stage is finished, the resulting state will have an internal energy and temperature distributions. These are used as the initial condition for the simulation of holding of the molten aluminum.

The holding chamber is filled with air in this part of the simulation; it is simulated along with all the other domains. The heat losses in walls and the heat input from the electrical resistances are taken into account by the boundary conditions explained above. The preheating process is accomplished until the temperature of the furnace walls becomes almost stable. Fig. 4 shows the temperature profile in the furnace estimated in the simulations of the quarter and full domain for the preheating stage.

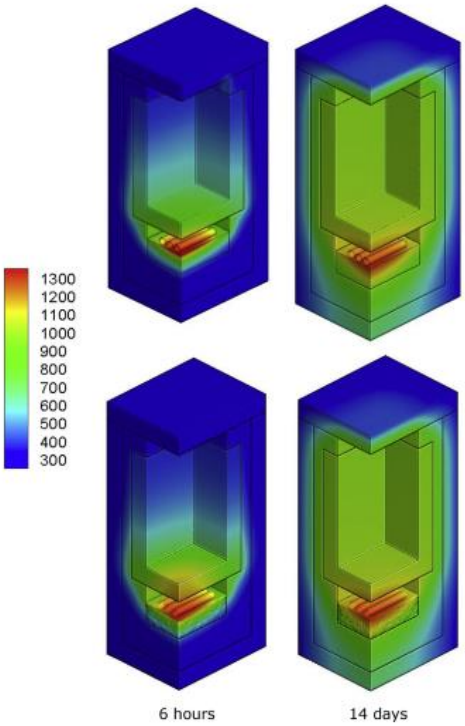

Fig. 4. Temperature for preheating stage [K]. Up: quarter of domain. Down: full domain.

Temperatures e holding process

After a stable solution from the preheating stage is obtained, the simulations are carried out for the holding process. In the real facilities, a load of 250 kg of aluminum is poured into the holding chamber in liquid state at 1023 K. Then, the molten load is maintained until the system achieves steady state. These conditions are reproduced in the numerical simulation. Results of the simulations show that the holding furnace can keep of the molten load at target temperature. Fig. 5 shows the temperatures predicted by the numerical approaches in the furnace and load for the holding process.
Fig. 6 shows a comparison between the numerical predictions and the experimental observation of the wall temperatures in the measurement points (T3-T5 in Fig. 1); in this graph, zero wall thickness indicates the internal wall and increases through the external refractory walls.
Figs. 4-6 show the great similarities in temperature estimates for quarter and full domains approaches. As is shown in Fig. 5, the temperatures in the load are very homogeneous; in fact, the difference between the maximum and minimum temperatures is always less than 5 K. The temperature difference between holding and resistance chambers is 200 K. According to the experimental temperature measurements shown in Fig. 6, the process was simulated within a reasonable agreement with real conditions considering the complexity of the simulation.

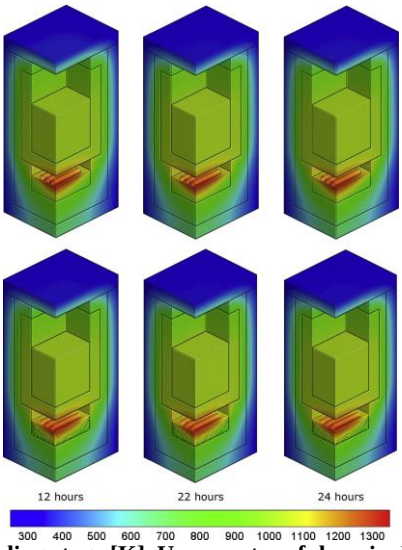

Fig. 5. Temperature for holding stage [K]. Up: quarter of domain. Down: full domain.

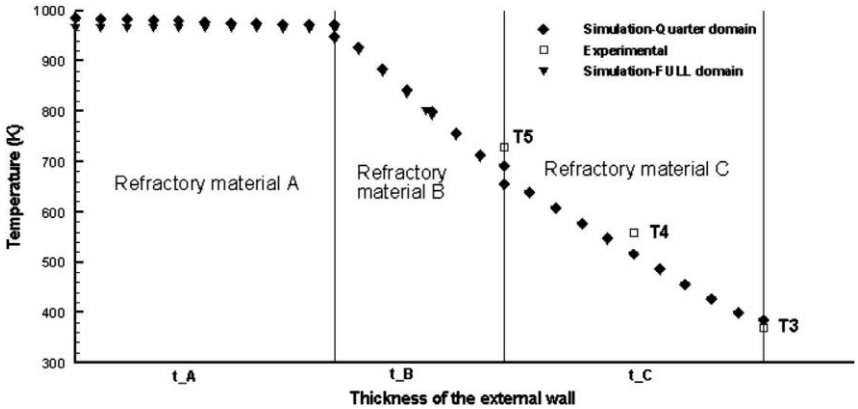

Fig. 6. Wall temperature profile - numerical estimations and measurements (T3-T5).

Convection effects

The homogeneity of the temperatures presented in this device is an effect highly desirable in aluminum holding furnaces [1], which is obviously enhanced by convection effects [24].

In the computations, even though the low variation in temperature inside the load and the almost constant condition of the refractory parts, it was not possible to obtain a steady state solution for velocity of the molten material. Fig. 7 shows the variation of several iso-surfaces of vertical velocity for the holding process.

The unsteady character of the movement in the molten load is manifest. The quarter of domain calculation predicts higher velocities than the full domain, off course with a symmetrical pattern. On the other hand, the full domain calculation predicts a pattern highly three dimensional. Therefore, in spite of the resemblance of the thermal performance estimated by both approaches, the internal flow is strongly limited by the symmetry simplifications. In order to determine the features of the flow, four control points are located on a plane at half height of the load: 1) center line of the furnace, 2) center of thin wall 3) corner of the furnace; 4) center of the thick wall. In each, Z-velocity (vertical velocity) and temperature are continuously registered for a representative simulation time. Fig. 8 shows the location of these control points in the quarter of domain.

Figs. 9 and 10 show the Z-velocities and temperatures registered respectively, in the control points for both the quarter and full domain calculations. Since the furnace operation is almost in steady state condition for the holding process, the measured temperature of the load (see T1 in Fig. 1) was conserved approximately constant throughout the test with a value of 1078 K. Predicted temperatures of the load for both numerical simulations have values ranging from 1045 to 1050 K. The difficulty on the temperature measurement for the molten load and the accuracy of the instrument makes not feasible to obtain experimentally the profiles presented in Fig. 10.

A pure periodic behavior is predicted by the simulations of the quarter of domain in each control point, whereas for the full domain also an oscillatory behavior is predicted, but in this case the signal is not purely periodical. Velocities in the molten load vary significantly between both simulations. Load temperatures estimated by the quarter of domain approach are slightly higher than that of the full domain approach; nevertheless the difference can be neglected in practical terms for industrial applications. In order to obtain the dominant frequencies in the flow of the molten load, the Fast Fourier Transform (FFT) [25] is applied to the registers in time of the Z-velocity and temperatures for each control point. They are shown in Figs. 11 and 12 respectively.

In accordance with previous observations, it is shown that the simulation of a quarter of domain tends to produce discrete frequency peaks, whereas the spectra are more continuous and rich when the full domain is considered. The oscillatory responses are not related to the on-off control mode that operates at much higher frequency (ca. 0.05e0.1 Hz).

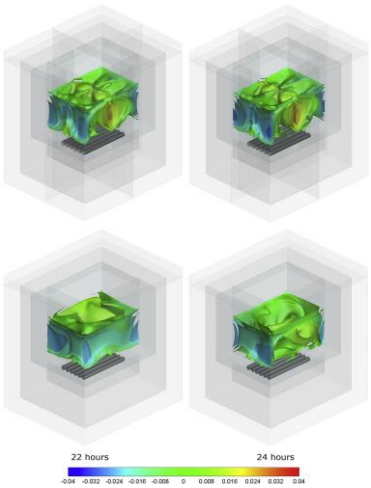

Fig. 7. Iso-surfaces vertical velocities for the molten aluminum. Up: quarter of domain. Down: full domain.

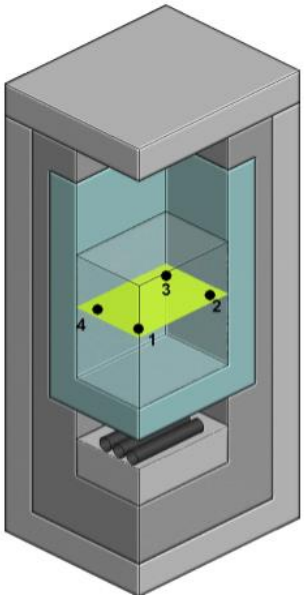

Fig. 8. Location of control points for the molten load.

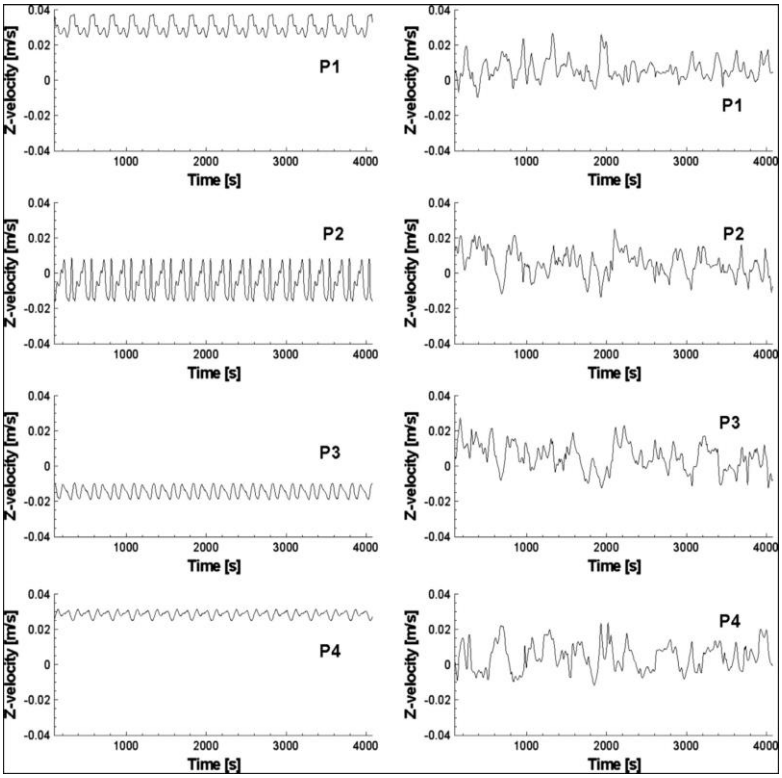

Fig. 9. Z-Velocities registered (m/s) in control points P1-P4. Left: quarter of domain. Right: full domain.

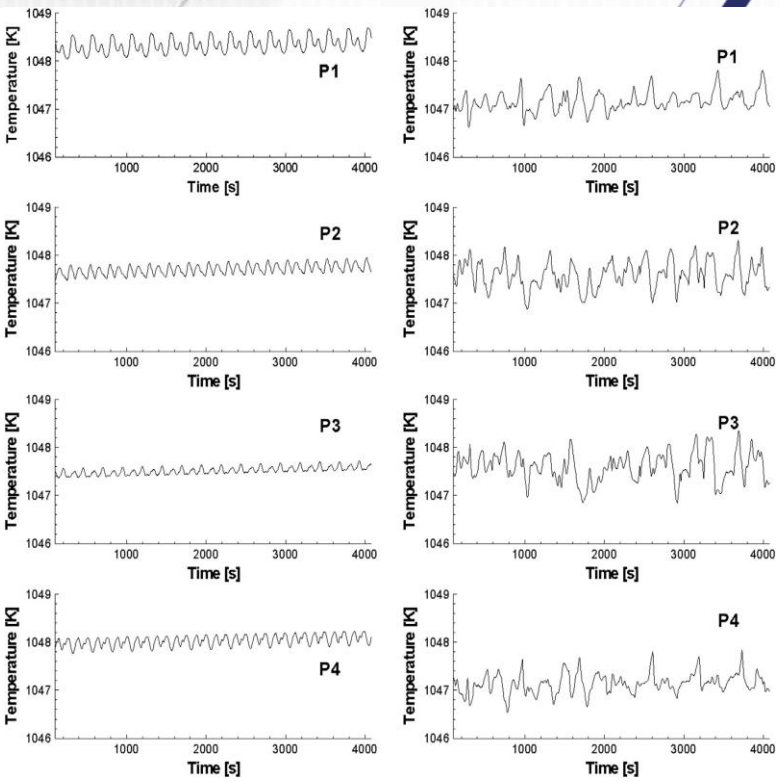

Fig. 10. Temperatures registered (K) in control points P1-P4. Left: quarter of domain. Right: full domain.

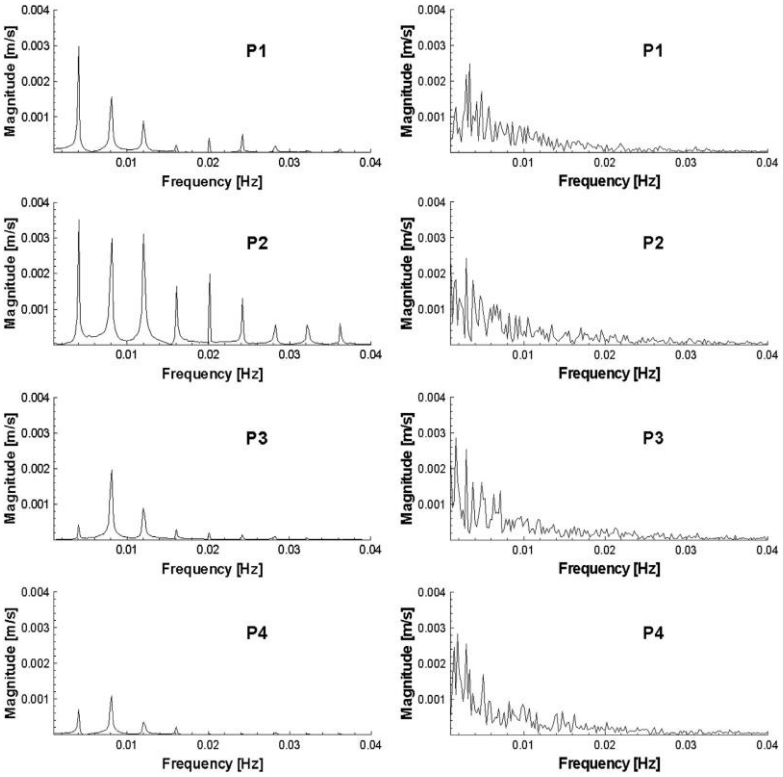

Fig. 11. FFT for Z-velocities registered in control points P1-P4. Left: quarter of domain. Right: full domain.

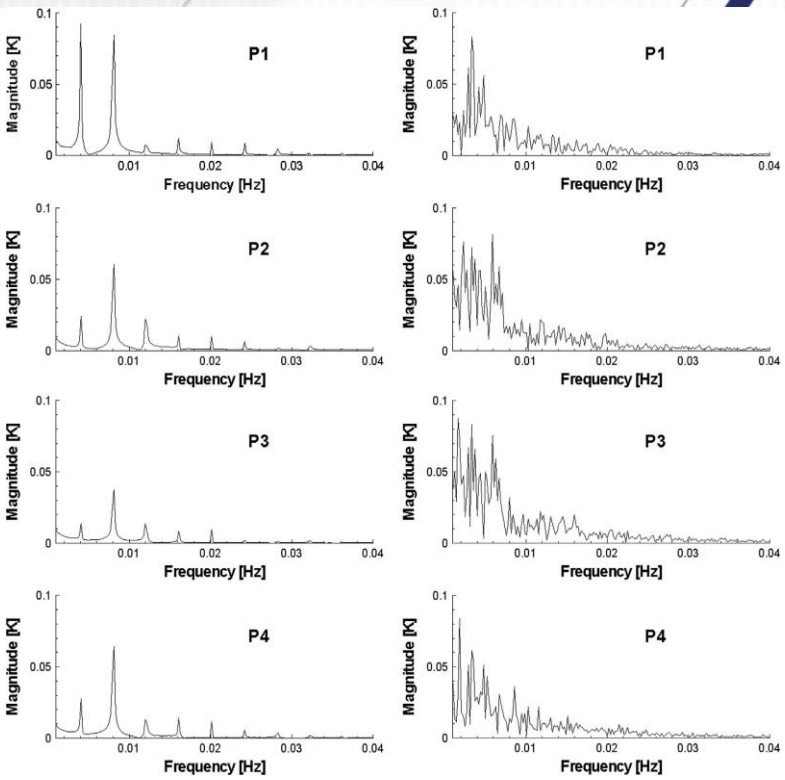

Fig. 12. FFT for temperatures registered in control points P1-P4. Left: quarter of domain. Right: full domain.

Discussion on velocity simulation results

In resemblance to these results, chaotic behavior is usually observed in natural-convection systems as a result of their intrinsic instability, see e.g. Gebhart [26]. It has been established that in natural convection problems the flow remains steady until a critical value of the Rayleigh number. When the Rayleigh number is increased several transitional regimes appear, from steady, including periodic, pseudo-periodic, chaotic and finally turbulent behavior. The transition of each stage is conditioned additionally by the fluid characteristics (Prandtl number).

At small Pr typical of liquid metals, the flow has been observed to be unsteady and finally turbulent at very low Rayleigh numbers. Since accurate measurements of velocities and temperature are very difficult for liquid metals, transitions between flow regimes are not yet completely understood. Due to the evident advantages of measurements at temperatures close to the ambient, some studies have been developed for mercury and gallium

(Pr = 0.02-0.025) in horizontal enclosures, in which a turbulent regimen appears for Ra > 2-4.

Discussion on velocity simulation results

The aim of the simulations presented here is the use of the models in industrial applications; these include a practical approach of the whole system, i.e. conjugated problem with refractory walls, heating means, heat losses, etc. Numerical literature of flows induced by natural convection considers simplified fluid-only domains with basic boundary conditions in order to make feasible smaller mesh sizes and achieve Direct Numerical Simulation (DNS) conditions, which is not the objective of this work. According for instance to the spatial resolution for a DNS of Grotzbach€ [27], the grid size for the load domain under the current conditions (Pr ~ 0.003 and Ra ~ 5e7), should be approximately of 1000*1750* 1223 elements instead of the 38* 66* 46 elements used here. Considering that the simulation of the holding furnace for the full domain approach has required 6 months of wall clock time, the recommended range for the spatial discretization in DNS to solve all the flows scales is prohibitively expensive for the current purposes (see also e.g. Chilla and Schumacher [28]).

It is thus clear that flow results of the simulations don't constitute a proper solution of the problem, since it has assumed unsteady (laminar) flow without enough spatial resolution to replicate the details.

However, thermal results appear perfectly reliable and useful for industrial application. On the other hand, the model can predict chaotic behavior, even for the full domain in a range of frequencies (no discrete frequencies), which is very curious and points to the field of Rayleigh-Benard flows. In this regard, some authors have presented their works in convection problems in liquid metals, especially for mercury and gallium. Verzicco and Camussi [29] present 3D numerical simulations of the transitions from the onset of convection to fully developed turbulence flow, in a cylindrical cell and in mercury; they found that the flow remained steady up to Ra ~ 2.11e4 when an oscillatory instability is observed. As the Rayleigh number is further increased, this oscillatory regime evolves towards a more complex state with more frequencies in the time oscillations (Ra ~ 2.75e4 – 3e4) and finally the turbulent state is achieved (Ra ~ 3.75e4), where the formation of more sub-harmonics tends to fill the spectrum. These flow regimes resemble the current predictions of periodic and chaotic movement obtained in the quarter and full domain calculations of the holding furnace, respectively.

These diverging results are obtained in the present work even though both simulations have the same Rayleigh number. This is difficult to explain, although it points to the difference in the aspect ratios (length/height), since the transition in flows also depends on the geometry of the fluid vessel, as is pointed out by Crunkleton et al. [30], who presented numerical simulations of the transition from steady to oscillatory flow for a very low Prandtl number fluid (Pr = 0.008) in rectangular enclosures with different aspect ratios; they found that flows in cavities with higher heights are more stable than those in geometries with high aspect ratios. This conclusion is in agreement with the results obtained here and it is supported by several authors, such as Puits et al. [31] or Bailon-Cuba et al. [32] in analysis with air, experimental and numerical respectively. Hof et al. [33] present an experimental and numerical simulation of the oscillatory convection in molten gallium for a rectangular cavity, where the metal is heated from lateral walls; they obtain oscillatory behavior for very low Rayleigh numbers. On the other hand, Lee and Park [34] have presented a 2D numerical analysis on natural convection in an enclosure having a vertical thermal gradient with a square insulator inside; with this configuration they obtained in a fluid with Pr = 0.01 periodic and pseudo periodic behaviors with Ra = 10^5 and Ra = 10^6 respectively. These studies encompass also simplified domains compared with the present holding furnace; but they indicate that a chaotic behavior is expected with the current conditions. In this sense, the assumption of a symmetry boundary condition in this kind of applications prevents the correct prediction of the convection effects due to suppression of three dimensional expansions.

In practical terms, the homogeneity of the temperature inside the load makes the current approaches good enough for industrial purposes. Nevertheless, it is necessary to take into account the convection effects in order to prevent over estimations of temperatures. Furthermore, in this kind of devices the movement of the load has important consequences in several aspects, e.g. the elimination of thermal gradients, that also lead to excessive dross formation and melt loss, inclusions, variable chemistry, and problems with casting when metal of varying temperatures is tapped. Also in some holding furnaces, the efforts to enhance mixing times are mandatory since one of the main purposes of the device is to adjust the composition with alloy elements; in such cases, the movement of the load affects directly the efficiency of the furnace [35]. It is clear that this effect would deserve more research and should be treated with more suitable models, but the limitations imposed for industrial applications require a compromise between accuracy and computational cost; in this sense, the unsteady, Reynolds averaged Navier-Stokes (URANS) methods include simplified turbulence models that could provide a good alternative to solve the full convection effects in these devices. The incorporation of this kind of models will be possible in a future with the increase of the computational resources.

Conclusions

- ✓ Detailed three dimensional, unsteady state simulations are presented with the purpose to estimate the thermal behavior of a holding furnace heated by electrical resistances; the simulations reproduce experimental tests in a real prototype. An exhaustive thermal simulation is intended, including models of heat conduction, convection, interactions of gas-liquid-solid zones and radiation heat transfer.

- ✓ Two cases of simulation are studied and their effects in results are evaluated. The first case takes advantage of the symmetric geometry and considers only a quarter of domain. The second case considers the full domain.
- ✓ Numerical simulations show that the holding furnace can keep the temperature of the molten load above the melting point. The temperatures predicted agree with measurements taken in a real prototype for a typical operation cycle. Temperature of the molten aluminum is almost uniform.
- ✓ However, the naturally induced velocity does not converge to a steady-state solution, exhibiting instead highly three dimensional, periodic and oscillatory behavior. Benchmarking with basic experimental and numerical data from the literature on liquid metals, it can be concluded that the real flow is very likely chaotic or even turbulent, so that our numerical approach cannot be considered a proper model.
- ✓ Nevertheless, predicted oscillations seem realistic and the issue apparently does not affect the industrial significance of the results. Also the flow differs greatly between the computation with imposed symmetry (quarter of domain) and the full domain calculation. Whereas the first is purely periodic, the second is more chaotic, with a richer velocity spectrum.

References

[1] J.M. Wang, S. Lan, W.K. Li, Numerical simulation and process optimization of an aluminum holding furnace based on response surface methodology and uniform design, Energy 72 (2014) 521-535.
[2] N.-j. Zhou, S.-h. Zhou, J.-q. Zhang, Q.-l. Pan, Numerical simulation of aluminum holding furnace with fluid-solid coupled heat transfer, J. Cent. South Univ. Technol. 17 (2010) 1389-1394.
[3] E. Pauty, B. Laboudigue, J. Etay, Numerical simulation of the flow and the solid transport when tilting a holding furnace, Metall. Mater. Trans. B 31 (2000) 207-214.
[4] S.M.H. Darwish, The finite-element modeling of aluminum holding furnaces, JOM 43 (1991) 36e38.
[5] S.G. Blakey, S.B.M. Beck, The effect of combined radiation and convection on hot dip galvanizing kettle wear, Appl. Therm. Eng. 24 (8) (2004) 1301-1319.
[6] E. Martín, M. Meis, C. Mourenza, D. Rivas, F. Varas, Fast solution of direct and inverse design problems concerning furnace operation conditions in steel industry, Appl. Therm. Eng. 47 (2012) 41-53.
[7] R.P. Mooney, S. McFadden, Z. Gabalcova, J. Lapin, An experimental-numerical method for estimating heat transfer in a Bridgman furnace, Appl. Therm. Eng.67 (1) (2014) 61-71.
[8] M. Carmona, C. Cortes, Numerical simulation of a secondary aluminum melting furnace heated by a plasma torch, J. Mater. Process. Technol. 214 (2014) 334-346.
[9] ANSYS, ANSYS FLUENT 14.0 User's Guide, 2012.
[10] A.F. Mills, Heat Transfer, Richard D. Irwin, United States of America, 1992.
[11] F.P. Incropera, D.P. De Witt, Fundamentals of Heat and Mass Transfer, third ed., John Wiley and Sons Inc., United States of America, 1990.
[12] Goodfellow, Catalogue: Goodfellow. www.goodfellow.com, (accessed12.11.14).
[13] Skamol, Catalogue: Skamol. www.skamol.com, (accessed 12.11.14).
[14] Dupre, Catalogue: Dupr - minerals. www.dupreminerals.com/en, (accessed 12.11.14).
[15] Christy, Catalogue: Christy refractories. www.christyco.com/refractories.html, (accessed 12.11.14).
[16] Rath, Catalogue: Rath. www.rath-usa.com/pds-ceramic-fiber-paper.html, (accessed 12.11.14).
[17] Outokumpu, Catalogue: Outokumpu VDM. www.thyssenkrupp-vdm.com, (accessed 12.11.14).
[18] MatWeb, MatWeb data base. www.matweb.com, (accessed 12.11.14).
[19] M.J. Assael, K. Kakosimos, R.M. Banish, J. Brillo, I. Egry, R. Brooks, P.N. Quested, K.C. Mills, A. Nagashima, Y. Sato, W.A. Wakeham, Reference data for the density and viscosity of liquid aluminum and liquid iron, J. Phys. Chem. Ref. Data 35 (2006) 285e300.
[20] J.L. Brandt, Properties of pure aluminum, in: J.E. Hatch (Ed.), Aluminum: Properties and Physical Metallurgy, American Society for Metals, Ohio, United States of America, 1984.
[21] H. Zeiger, H. Nielsen, Constitucion y propiedades de los materiales de aluminio, in: W. Hufnagel (Ed.), Manual del aluminio, vol. 1, Reverte, Barcelona, Espana, 200~ 4.

[22] V. Voller, A. Brent, K. Reid, Computational Modelling Framework for Analysis of Metallurgical Solidification Processes and Phenomena, The Institute of Metals, 1988, pp. 378-380.
[23] V.R. Voller, M. Cross, N.C. Markatos, An enthalpy method for convection/ diffusion phase change, Int. J. Numer. Methods Eng. 24 (1987) 271-284.
[24] A. Tripathi, J.K. Saha, J.B. Singh, S.K. Ajmani, Numerical simulation of heat transfer phenomenon in steel making ladle, ISIJ Int. 52 (2012) 1591-1600.
[25] E.O. Brigham, the Fast Fourier Transform and its Applications, Prentice Hall, United States of America, 1988.
[26] B. Gebhart, Y. Jaluria, R.L. Mahajan, B. Sammakia, Buoyancy-induced Flows and Transport, Hemisphere Publishing Corporation, United States of America, 1988.
[27] G. Gro€tzbach, Spatial resolution requirements for direct numerical simulation of the Rayleigh-Benard convection, J. Comput. Phys. 49 (1983) 241-264.
[28] F. Chilla, J. Schumacher, New perspectives in turbulent Rayleigh-Benard convection, Eur. Phys. J. E 35 (2012) 1-25.
[29] R. Verzicco, R. Camussi, Transitional regimes of low-Prandtl thermal convection in a cylindrical cell, Phys. Fluids 9 (1997) 1287-1295.
[30] D.W. Crunkleton, R. Narayanan, T.J. Anderson, Numerical simulations of periodic flow oscillations in low Prandtl number fluids, Int. J. Heat Mass Transfer 49 (2006) 427-438.
[31] R.d. Puits, C. Resagk, A. Thess, Thermal boundary layers in turbulent Rayleigh-Benard convection at aspect ratios between 1 and 9, New J. Phys. 15 (2013) 013040.
[32] J. Bailon-Cuba, M.S. Emran, J. Schumacher, Aspect ratio dependence of heat transfer and large-scale flow in turbulent convection, J. Fluid Mech. 655 (2010) 152-173.
[33] B. Hof, A. Juel, L. Zhao, D. Henry, H.B. Hadid, T. Mullin, On the onset of oscillatory convection in molten gallium, J. Fluid Mech. 515 (2004) 391-413.
[34] J.R. Lee, I.S. Park, Numerical analysis for Prandtl number dependency on natural convection in an enclosure having a vertical thermal gradient with a square insulator inside, Nucl. Eng. Technol. 44 (2012) 283-296.
[35] M.E. Schlesinger, Aluminum Recycling, Taylor & Francis, United States of America, 2006.